BACTERIALLY INDUCED MINERALIZATION OF CALCIUM CARBONATE IN TERRESTRIAL ENVIRONMENTS: THE ROLE OF EXOPOLYSACCHARIDES AND AMINO ACIDS

OLIVIER BRAISSANT, GUILLAUME CAILLEAU, CHRISTOPHE DUPRAZ, AND ERIC P. VERRECCHIA
Institut de Géologie, Université de Neuchâtel, Rue Emile-Argand 11, CH-2007 Neuchâtel, Switzerland
e-mail: eric.verrecchia@unine.ch

ABSTRACT: **This study stresses the role of specific bacterial outer structures (such as glycocalix and parietal polymers) on calcium carbonate crystallization in terrestrial environments. The aim is to compare calcium carbonate crystals obtained in bacterial cultures with those obtained during abiotically mediated synthesis to show implications of exopolysaccharides and amino acids in the mineralogy and morphology of calcium carbonate crystals produced by living bacteria. This is done using various amounts of purified exopolysaccharide (xanthan EPS) and L-amino acids with a range of acidities. Amino acids and increasing xanthan content enhance sphere formation in calcite and vaterite. Regarding calcite, the morphology of crystals evolves from rhombohedral to needle shape. This evolution is characterized by stretching along the *c* axis as the amino acid changes from glutamine to aspartic acid and as the medium is progressively enriched in EPS. Regarding vaterite, the spherulitic habit is preserved throughout the morphological sequence and starts with spheres formed by the agglomeration of short needles, which are produced in a xanthan-free medium with glutamine. Monocrystals forming spheres increase in size as xanthan is added and the acidity of amino acids (glutamic and aspartic acids) is increased. At high xanthan concentrations, amino acids, and mainly aspartic and glutamic acids, induce vaterite precipitation. The role of the carboxyl group is also probably critical because bacterial outer structures associated with peptidoglycan commonly contain carboxyl groups. This role, combined with the results presented here, clearly demonstrate the influence of bacterial outer structure composition on the morphology and mineralogy of bacterially induced calcium carbonate. This point should not be neglected in the interpretation of calcite cements and carbonate accumulations in terrestrial environments.**

INTRODUCTION

Microbiologically induced mineralization is defined as processes leading to inorganic mineral deposits by adventitious precipitation. This precipitation arises from secondary interactions between various metabolic processes producing carbonate species and the surrounding environment (Mann 2001). Mineral precipitation by microbes has been known about for a long time (see historical aspects in Ehrlich 1996, 1998). Among bacterially precipitated minerals, carbonates, and in particular calcium carbonate ($CaCO_3$) in numerous forms, are probably the most important (Ferris et al. 1989). Bacterially precipitated calcite (in terrestrial environments), and aragonite and high Mg calcite (in marine environments) have been described many times in the literature (e.g., Boquet et al. 1973; Castanier et al. 2000; Chafetz 1986; Krumbein 1979). Although other species of calcium carbonate minerals are only rarely associated with bacterial activity, there are a couple of recently described examples: vaterite precipitation by the soil bacteria *Xanthobacter autotrophicus* (Braissant et al. 2002; Braissant and Verrecchia 2002) and monohydrocalcite ($CaCO_3 \cdot H_2O$) by the halophilic bacteria *Halomonas eurihalina* (Rivadeneyra et al. 1998). The ecology of the microbes associated with vaterite and monohydrocalcite is consistent with the lacustrine environment in which the crystals formed (Giralt et al. 2001; Krumbein 1975) and not due to the activity of exotic strains under exceptional conditions. To our knowledge, microbially induced ikaite ($CaCO_3 \cdot 6H_2O$) has not been reported, probably because of its instability.

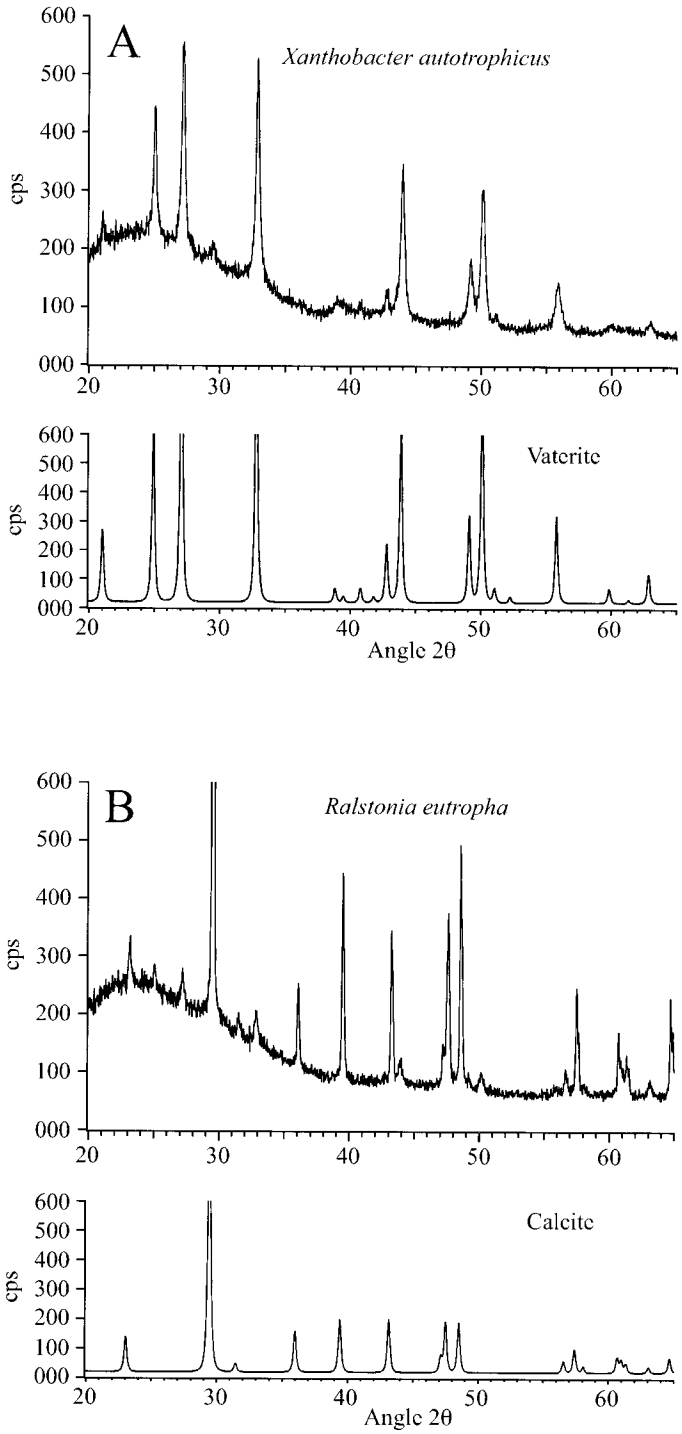

FIG. 1.—X-ray diffractograms of $CaCO_3$ crystals associated with **A)** *Xanthobacter autotrophicus* and **B)** *Ralstonia eutropha* cultures. These diffractograms correspond perfectly to vaterite (A) and calcite (B), respectively.

JOURNAL OF SEDIMENTARY RESEARCH, VOL. 73, NO. 3, MAY, 2003, P. 485–490
Copyright © 2003, SEPM (Society for Sedimentary Geology) 1527-1404/03/073-485/$03.00

Dolomite ($CaMg(CO_3)_2$) has been reported by Warthmann et al. (2000) to be precipitated by *Desulfonatovibrio* in anoxic marine environments.

Despite numerous reports of calcium carbonate precipitation by microbes and the important biomass they represent in soils, accumulation of terrestrial carbonates is still generally attributed to physicochemical processes (Lal et al. 2000). In this paper, it is demonstrated that relationships between morphologies and mineralogies of $CaCO_3$ encountered in soils and surficial sediments reveal a bacterial influence related to microbial biofilms. This study stresses the role of a specific exopolysaccharide (xanthan EPS) and amino acids on calcium carbonate crystallization in terrestrial environments.

In marine environments, outer structures such as the cyanobacterial S-layer have already been recognized as the main crystalline biostructure able to act as a nucleus for calcium carbonate growth (see review in Schultze-Lam et al. 1992, 1996 and Smarda et al. 2002). Most microbial cells in natural environments form communities inside microbial biofilms (Decho 1990, 2000; Sutherland 2001 a, 2001 b). Therefore, exopolysaccharides (EPS) and amino acids most likely play an essential role in calcium carbonate morphology and mineralogy. This study investigates the potential relationships between EPS, amino acids, oxidative soil bacteria, and calcium carbonate crystals using conventional bacterial cultures and abiotically mediated calcium carbonate synthesis. The aim is to compare calcium carbonate crystals obtained in bacterial cultures with those obtained during abiotically mediated synthesis. This is done using various amounts of purified EPS and L-amino acids with a range of acidities and frequently associated with mucilages.

MATERIALS AND METHODS

Bacterially mediated calcium carbonate crystals were obtained after 20 days culturing of *Xanthobacter autotrophicus* (syn: *Corynebacterium autotrophicum,* DSM 432, ATCC 35674) and *Ralstonia eutropha* H16 (syn: *Alcaligenes eutrophus,* DSM: 428, ATCC 17699) on a B4 medium kept at 26°C (Merck yeast extract 4.0 g/L; Merck calcium acetate 2.5 g/L; Merck agar-agar 15 g/L: Boquet et al. 1973). These two strains are oxidative terrestrial bacteria commonly found in soils and sediments. In the cultures, the main difference between the two strains is the amount of polysaccharide produced: *X. autotrophicus* is surrounded by a large amount of slime, whereas *R. eutropha* produces only an extremely low amount of glycocalix (Holt et al. 1993). The pH was not monitored during culturing, but final pH was > 9 as revealed by a droplet of pH indicator. Uninoculated Petri dishes were kept as a sterility control.

Abiotically mediated crystals have been obtained by precipitation from a $CaCl_2$ / $(NH_4)_2CO_3$ reaction inside a polysaccharidic medium (EPS) with various types of L-amino acids. The aim of this experiment is to simulate precipitation of calcium carbonate in an EPS-rich environment without involving living bacteria. Ten runs of this experiment have been conducted. The synthesis was performed using a $CaCl_2$ 0.05 M solution to which was added: (1) 1.0% (w/v) amino acids (L-glutamine, L-glutamic acid and L-aspartic acid. These amino acids were chosen because they are commonly found in the parietal structures of many bacteria, e.g. polyglutamate in *Bacillus anthracis, Mycobacterium tuberculosis, Sporosarcina halophila,* polyglutamine in the genus *Xanthobacter* and *Flexithrix,* and finally polyaspartate in *Synechococcus sp.*); and (2) 0%, 0.1%, 0.5% and 1.0% (w/v) concentrations of xanthan from Sigma™ (a bacterial EPS mainly composed of mannose and glucose). The pH of this solution was adjusted to 8.4 (the pH of calcite stability at 1 atm and 25°C) before adding xanthan. The solution was sterilized by autoclaving at 121°C for one hour. After sterilization, the solutions were placed in Petri dishes that remained for 20 days in ethanol-washed desiccators filled with $(NH_4)_2CO_3$. Petri dishes were examined with a binocular microscope to control possible presence of contaminants.

Crystals obtained in bacterial cultures, as well as in the abiotic experiment, were both isolated by either sedimentation or directly from the culture using precision tweezers. The crystals obtained were gold coated and observed with a Philips XL20 SEM. Crystals sampled from bacterial colonies were previously washed in saturated calcium hypochlorite solution in order to remove organic matter from the surfaces of the crystals. Samples of bacterial colonies bearing crystals were fixed with glutaraldehyde (5%), immediately dehydrated in ethanol, and air-dried after ethanol replacement by tetramethylsilane (TMS; Dey et al. 1989). These samples were gold sputter coated for 60 seconds to give a 23 nm gold coating, and observed with a Philips XL20 SEM. Crystals were analyzed by X-ray diffraction (XRD) using a Scintag diffractometer and by an energy-dispersive spectrometry (EDS) microprobe coupled with a Philips XL30 environmental scanning electron microscope (ESEM). Calcite and vaterite mineralogies were determined by cross checking XRD analyses, crystal habits, and relative proportions of each phase plus comparison of observed crystal shapes with shapes documented in the literature.

RESULTS

Calcium Carbonate Crystals Obtained in Bacterial Cultures

Bacterially mediated crystals were found mostly on the surfaces of colonies. They have various mineralogies and morphologies. In terms of mineralogy, *X. autotrophicus* produced mainly brown vaterite spherulites ranging from 50 μm to 200 μm in diameter, with a small fraction of calcite crystals (Fig. 1A), whereas *R. eutropha* produced colorless calcite crystals ranging from 100 μm to 600 μm in size, with traces of vaterite (Fig. 1B).

Spheres produced by *X. autotrophicus* show three different monocrystal (small individual crystal) arrangements (Fig. 2A–D). Although the overall sphere shape remains, the morphology of individual crystals forming the sphere varies from a fan shape to a needle (Fig. 3). The crystals are organized around a central point and grow radially to form the sphere. Accessory shapes are also associated with the spheres. They are made of either a polyhedral assemblage of calcite crystals or a mixture of calcite and vaterite. Two main morphologies have been observed. ''Fried egg'' shapes are probably formed at the surface of the colony (Fig. 2E–G). The subspherical part is constituted by vaterite and grows on a lens- to plate-shape calcite surface. The flat part is in contact with the atmosphere, the sphere being inside the colony. Therefore, the general shape is a flipped ''fried egg.'' Calcite also forms imperfect spherical clusters made of imbricated rhombohedra (Fig. 2H).

→

FIG. 2.—Morphology of crystals obtained during bacterial growth. A–H, *Xanthobacter autotrophicus* ; I–P, *Ralstonia eutropha*. **A**) General view of vaterite spherulites in cross-polarized light (XPL). **B**) Close-up of part A showing two different crystal arrangements. Spheres showing a black cross are constituted by needles, whereas other spheres are formed by clusters of small monocrystals. **C, D**) Scanning electron microscope (SEM) view of individual (C) and coalescent (D) vaterite spherulites. The surface of the sphere is not smooth and shows a mammillated rough topography. **E, F**) ''Fried egg'' morphology of accessory crystals. These clusters are constituted by two parts, a calcitic bottom part having a lens- to plate-shape and a central hemispherical upper part constituted by vaterite crystals of various sizes. **G**) Detail of the hemispherical part showing small hexagons of vaterite. **H**) Imbricated rhombohedra forming imperfect spherical calcite clusters. **I**) Subhedral to euhedral rhombohedra. XPL view. **J**) ESEM view of a calcite flower formed by flat sparitic crystals. **K**) SEM view of the heart of a calcite flower constituted by crystals forming a spiral-like structure. **L**) SEM view of a calcite flower with petals formed by thin palissadic crystals. **M**) XPL view of a calcite cluster constituted by four triangular-shaped crystals joined at their tip to form a thickened Maltese cross. **N**) SEM view of a similar crystal shown in part M. **O, P**) XPL and SEM view of funnel-like crystals.

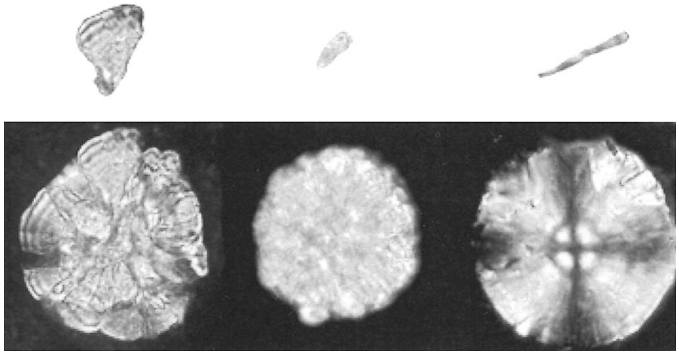

FIG. 3.—Morphology of individual crystals forming calcium carbonate spheres associated with *Xanthobacter autotrophicus*. From left to right: fan-shaped, petal-like, and needle monocrystals. The two first spheres are vaterite, and the third is either calcite or vaterite.

Crystals produced by *R. eutropha* have three main shapes. The two most common morphologies encountered are euhedral to subhedral rhombohedra (Fig. 2I) and calcite flowers, composed of crystals with euhedral terminations (Fig. 2J–L). The center of the flower is formed by a circular spiral-like crystal (Fig. 2K). Two other shapes have been observed: thickened ''Maltese crosses'' (Fig. 2M, N) and, rarely funnels (Fig. 2O, P). In blank uninoculated Petri dishes, crystals were not observed, emphasizing the crucial role of bacteria.

Calcium Carbonate Crystals Obtained in Abiotically Mediated Experiments

The reaction between $CaCl_2$ and $(NH_4)_2CO_3$, with neither xanthan nor amino acids present, produces calcite rhombohedra (Fig. 4A), which is not surprising. However, synthesis of calcium carbonate crystals in mucilaginous solutions results in numerous crystal morphologies, emphasizing the potential role of EPS in their shape diversity. Synthesis using increasing concentrations of xanthan without the addition of amino acids leads mainly to individual and branching crystals. At a low concentration of xanthan (0.1%), dendritic crystals form. Dendrites can be disordered, and similar to structures obtained by diffusion-limited aggregation (Fig. 4B), or ordered along the main three directions of calcite crystal growth (Fig. 4B). Nevertheless, subhedral rhombohedra remain the most abundant shape (Fig. 4B). At a higher concentration of xanthan (0.5%), the most common shape (constituting about 90%) is a dendrite-like crystal, which is in fact lacunar and made of small stacked rhombohedra (Fig. 4C). Around 5% of the crystals are euhedral rhombohedra (Fig. 4C). The remaining 5% are imbricated rhombohedron twins that form irregular spheroidal clusters (Fig. 4C). When the xanthan concentration reaches 1%, more and more imbricated rhombohedron twins agglomerate until they form subspherical clusters. Whatever the concentration in xanthan, all the crystals obtained in the amino acid free media are calcitic.

When amino acids are added to the medium, various crystal morphologies are obtained (Fig. 4E–P). At first glance, it is difficult to clearly see a trend in morphologies, although the habit becomes more spherical as xanthan increases. In addition, the two calcium carbonate polymorphs—vaterite and calcite—are always precipitated during abiotic synthesis in the presence of amino acids. Nevertheless, the ratio between the two mineralogical species seems to be essentially related to the abundance of EPS and the nature of amino acids. Aspartic acid, glutamic acid, and glutamine always induced vaterite formation at a high concentration of xanthan (1.0%), although calcite is still present. Consequently, it is critical to discriminate between the two mineralogies in order to understand the difference in shapes in Figure 4. Two morphological sequences (Fig. 5) can be described in relation to increasing EPS content (which acts as a weak acid) and the acidity of the added amino acid. Glutamine is considered as a basic amino acid, whereas glutamic and aspartic acids are acidic, aspartic acid being more acidic than glutamic acid.

Regarding calcite (Fig. 5), the morphological sequence starts with rhombohedra produced in a xanthan-free medium with glutamine (Fig. 4E). The conditions in this case are the most basic (highest pH) of the total experiment involving amino acids. By adding xanthan and by increasing the acidity of amino acids (glutamic and aspartic acids), rhombohedron edges become smoother (Fig. 4G) and crystals form numerous twins, agglomerated around a center (Fig. 4G, H), and finally evolve to fibro-radial spheres (Fig. 4K–P). This sequence can be summarized by the decrease of the monocrystal size forming the shape, from calcite rhombohedra to calcite styloids followed by needles (Fig. 5).

Regarding vaterite (Fig. 5), the spherulitic habit is preserved throughout the morphological sequence. It starts with spheres formed by the agglomeration of short needles, which are produced in a xanthan-free glutamine medium (Fig. 4E). Nevertheless, some spheres are composed of larger (but still small) monocrystals (Fig. 4E). These monocrystals increase in size as xanthan is added and the acidity of amino acids (glutamic and aspartic acids) is increased (Fig. 4I, J, L–P). Contrary to the sequence described for calcite, the vaterite sequence can be illustrated by the increase in the size of the monocrystals forming the spheres. Nevertheless, in the presence of glumanine and glutamic acid and a high amount of EPS, vaterite can form fibro-radial spherulites, which show a black cross in polarized light, as shown by Dedek (1966). The only way to differentiate calcite from this vaterite is by using XRD.

←

FIG. 4.—Scanning electron microscope photographs of crystal morphologies obtained during abiotically mediated synthesis of calcium carbonate in the presence of exopolysaccharides and amino acids. Abscissa: Blank (no amino acids present), Gln, L-glutamine, Glu, L-glutamic acid, Asp, L-aspartic acid. Coordinates: xanthan content (a glucose and mannose polymer), from 0.0% (absence of xanthan) to 0.1, 0.5 and 1.0% w/v. **A**) Euhedral calcite crystals. **B**) Subhedral and dendritic calcite crystals. Dendritic crystals show two different morphologies: diffusion-limited aggregation clusters and ordered dendrites. **C**) Crystal morphologies become chunkier, leading to imbricated twins. Some euhedral rhombohedra are preserved. **D**) Agglomerated twins tending to form spheres. **E**) Euhedral calcite rhombohedra associated with vaterite spherulites composed of either short needle monocrystals or an agglomerate of small euhedral crystals. **F**) Imperfect calcite rhombohedra are present with vaterite spheres. General structure of vaterite spherulites is similar to part E. **G**) Rare spherulitic vaterite associated with calcite rhombohedra. Edges of calcite crystals are smoother than in part A, and they tend to form imbricated twin clusters. **H**) Vaterite and calcite spherulites. Calcite appears as imbricated twin clusters. In addition, both vaterite and calcite can be characterized by fibro-radial spheres. **I**) Upper part: vaterite spiky agglomerates and cauliflower-shaped calcite. Bottom part: left, calcite rhombohedra; right, epitactic growth of a hexagonal vaterite crystal on a calcite substrate forming cauliflower clusters. **J**) Spiky agglomerate of vaterite starting to form a sphere, and a rough calcite spherulite. **K**) Calcite spheres. The arrow shows remains of a rhombohedron emphasizing the transition between imbricated twin clusters shown in parts G and H and the structure of spheres formed by styloidic crystals. Double sphere of calcite showing a structure close to fibro-radial spheres and composed by styloidic monocrystals. **L**) Fibro-radial calcite and vaterite spheres with a smooth surface associated with spiky vaterite spherulites (arrow). **M**) Fibro-radial calcite spherulites (right). Spiky vaterite agglomerate (left). **N**) General view of spiky vaterite spherulites associated with calcite spheres. Flat shapes are due to contact of the surface of the medium with the atmosphere. **O**) Calcite spheres. Some spheres are constituted by stacked flat monocrystals, which can be compared with spheres formed by styloidic crystals shown in part K. **P**) General view of vaterite and calcite spheres. Vaterite spherulites are characterized by the agglomeration of large monocrystals, whereas calcite spheres are smooth and fibro-radial.

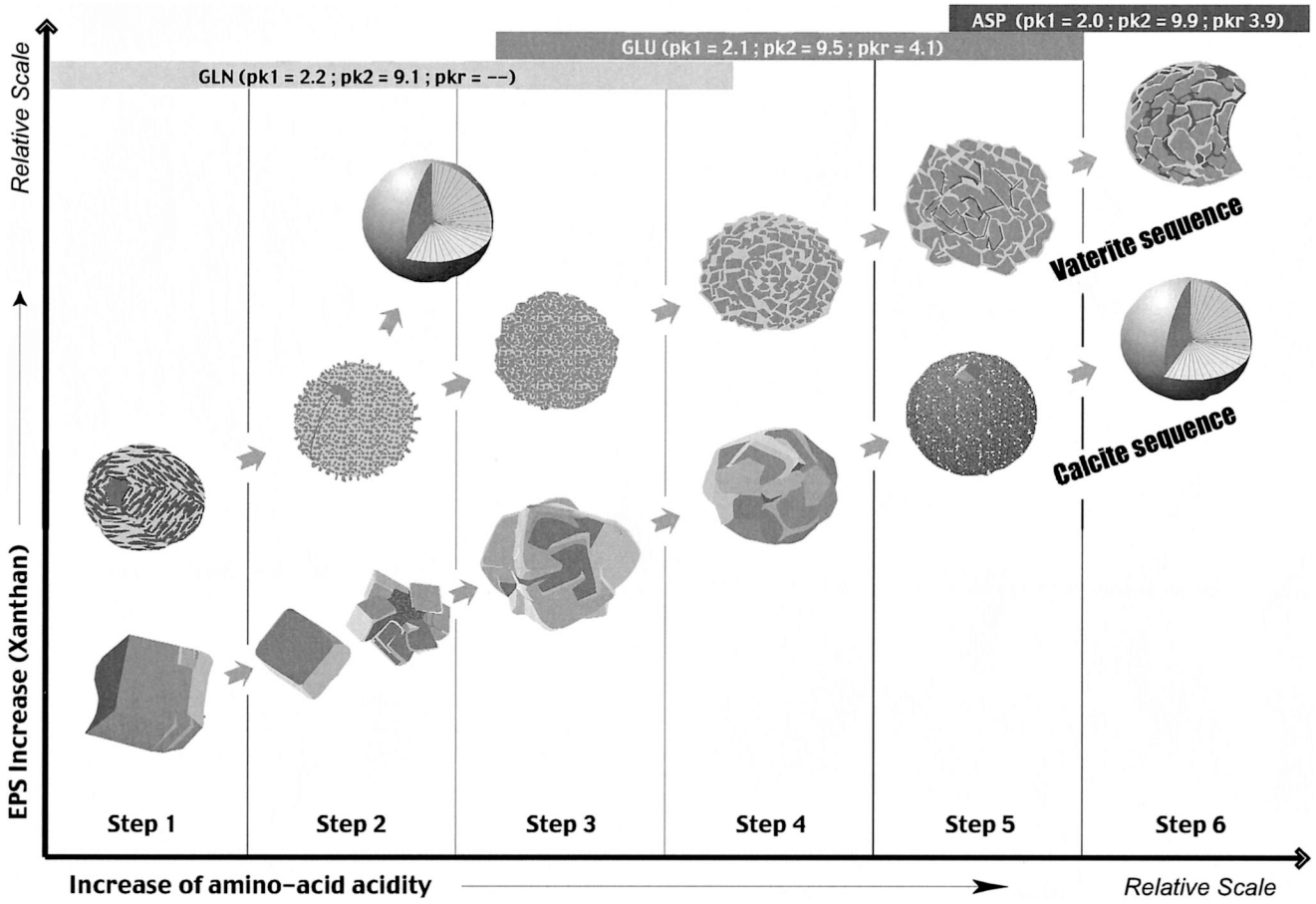

FIG. 5.—Sequences of calcite and vaterite morphologies obtained during the abiotic experiment. This sketch shows the morphologies related to increasing amino acid acidity and xanthan content. Scales are relative. The various domains of influence of amino acids are shown. Six main steps can be described for both vaterite and calcite. The calcite sequence starts with rhombohedra. Size of monocrystals forming the clusters decreases from Step 1 to Step 6 until they form needles. The general shape of calcite evolves from rhombohedra to fibro-radial spherulites. Vaterite sequence: vaterite is always precipitated as spheres. The monocrystals constituting the spheres increase in size from Step 1 (short needles) to Step 6 (large hexagons). Between Step 2 and Step 3, vaterite can occur as fibro-radial spherulites. Sketches were traced from photographs.

In summary, amino acids and increasing xanthan content enhance sphere formation in both calcite and vaterite. In addition, regarding calcite, the morphology of rhombohedra evolves from a euhedral shape to a needle. This evolution is characterized by stretching along the *c* axis as the amino acid changes from glutamine to aspartic acid and as the medium is progressively enriched in EPS.

DISCUSSION

Many spherulitic features are observed in carbonate soils and surficial sediments. The explanation of their origin is often unclear and usually attributed to possible organic influence without further elucidation. Spherulitic or oolitic habit have been observed in many other cases involving different microorganisms and different mineral species (e.g., Folk 1993). Calcium carbonate spherulites remain the most commonly described features. It has been shown that formation of aragonitic spherulites by *Deleya halophila* may be the result of cell calcification and aggregation (Rivadeneyra et al. 1996). In addition, formation of magnesian calcite spherulites and dumbbells has been related to the slime-producing bacteria, *Myxococcus xanthus* (González-Muñoz et al. 2000; Holt et al. 1993). Various types of apatite $[Ca_{10}(PO_4)_{6-x}(CO_3)_x(F,OH)_{2+x}]$ have been shown to precipitate with a spherulitic habit when under the influence of organic matter or during (nano)bacterial activity. Kajander and Çiftçioglu (1998) have shown that nanobacteria can be responsible for the formation of small spherulites (about 2 μm in diameter) alone or inside human cells (the spherulitic habit is not surprising considering the high density of macromolecules). Apatite spherulites including proteins (referred to as nanoforms) have also been shown to precipitate in a medium containing sterile fetal bovine serum (Vali et al. 2001). Salt ooids have been attributed to halophilic bacterial activity, which may guide the growth of biominerals (Castanier et al. 1999). In conclusion, recent research illustrates the numerous possible interactions between crystals and organic matter. Our results emphasize the importance of bacterial biofilms containing exopolysaccharides and amino acids in the precipitation of $CaCO_3$, and resemble features encountered in bacterial cultures, soils, and paleosols.

The morphologies of crystals obtained in *X. autotrophicus* and *R. eutropha* cultures (Fig. 2) can now be understood given the results depicted in Figure 4. *Xanthobacter autotrophicus* is known to produce substantial amounts of exopolysaccharides (Wiegel 1991). This property leads to the precipitation of vaterite spherulites (Fig. 2A–D), with some spheres showing a black cross of extinction in cross-polarized light. These morphologies are equivalent to those observed in Step 3 of Figure 5. Vaterite spherulites showing a black cross have also been observed, although rarely in the presence of glutamine with 0.5% xanthan. Regarding calcite, the accessory shape constituted by imbricated rhombohedra (Fig. 2H) is also equivalent to Step 3 of Figure 5. These observations indicate that crystals observed in the *X. autotrophicus* culture should be produced in a medium enriched

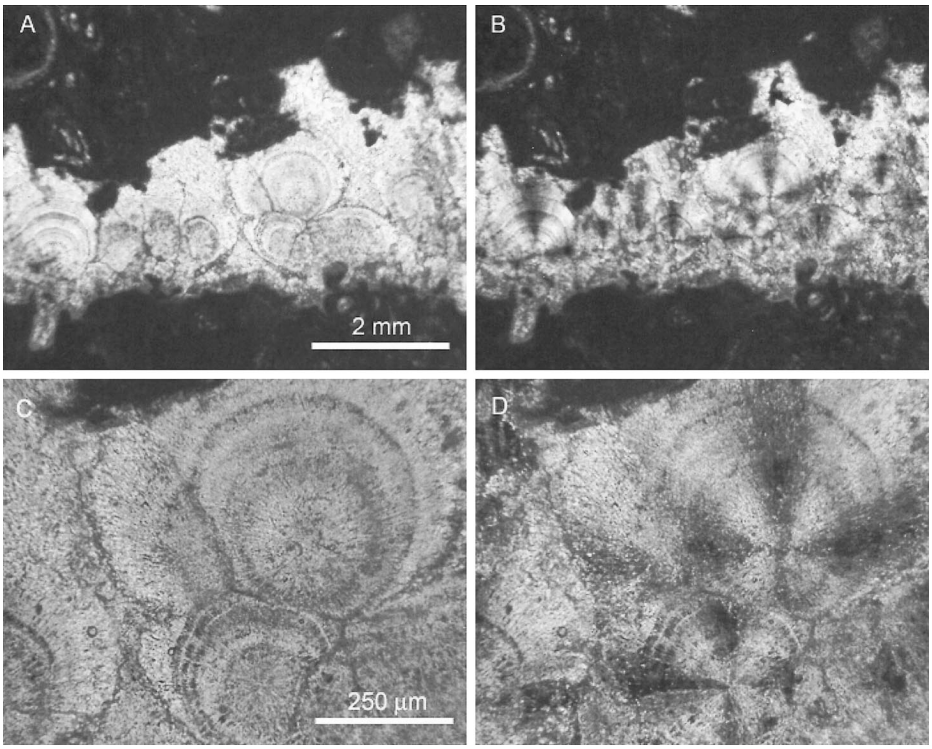

FIG. 6.—Spherulites associated with a paleosol in Bahamian eolianites (sample obtained by courtesy of C. Nawratil, University of Geneva). **A**) General view in plane-polarized light (PPL) of a planar pore infilled with a spherulitic calcite cement. **B**) Same view in cross-polarized light (XPL) showing the black cross of calcite spherulites. **C, D**) Detail in PPL and XPL of calcite spherulites showing some growth increments emphasized by impurities (organic matter) layers. These spherulites are virtually identical to those obtained in the presence of bacterial exopolysaccharides and amino acids.

in EPS as well as glutamine. Indeed, *X. autotrophicus* makes not only large amounts of exopolysaccharides but also a polyglutamine parietal polymer (Kandler et al. 1983; Wiegel 1991).

In contrast, the fact that *R. eutropha* only produces calcite rhombohedra and flower-shaped agglomerates is linked to an absence or only 0.1% EPS in the medium. The calcite crystals can be compared with Step 1 of calcite in Figure 5 or with crystals shown in Figures 4E and F. This is consistent with the fact that *R. eutropha* produces only low amounts of EPS.

The results obtained in Figure 4 can also be compared with features observed in natural environments. Spherulites showing an extinction cross in cross-polarized light are commonly found in soils and paleosols (Fig. 6). These spherulites infill pores and are associated with micritic and/or organo-micritic layers (Fig. 6A, B). Their origin has never been clearly identified. Nevertheless, their morphology (Fig. 6C, D) is identical to crystals produced in the EPS-rich medium (Fig. 4H, K, L, P). This point indicates the influence of biofilms in the precipitation of such spherulites in soils. A similar calcium carbonate spherulite has also been observed in a polysaccharide-rich tropical soil (Fig. 7A). Calcite and vaterite spherulites have also been reported in the mucilagenous sheath of cyanobacteria, indicating the fundamental role exopolysaccharides can play in their precipitation (Verrecchia et al. 1995; Giralt et al. 2001). In a different tropical soil, a feature identical to those shown in Figures 4J, M, and N has also been observed: it is a vaterite cluster growing on a quartz grain in a biofilm rich in EPS and amino acids (Fig. 7B). In conclusion, the abiotic experiments conducted in this study shed new light on the potential contribution of bacterial EPS and amino acids on calcium carbonate precipitation in terrestrial environments.

In natural environments, the variation of $CaCO_3$ crystal morphologies and mineralogies associated with EPS may result from its heterogeneity due to the diversity of microorganisms living within a single biofilm. Heterogeneity in slimes leads to differences in diffusion coefficients (local supersaturation), surface tensions, and viscosity. The viscosity of the 1.0%

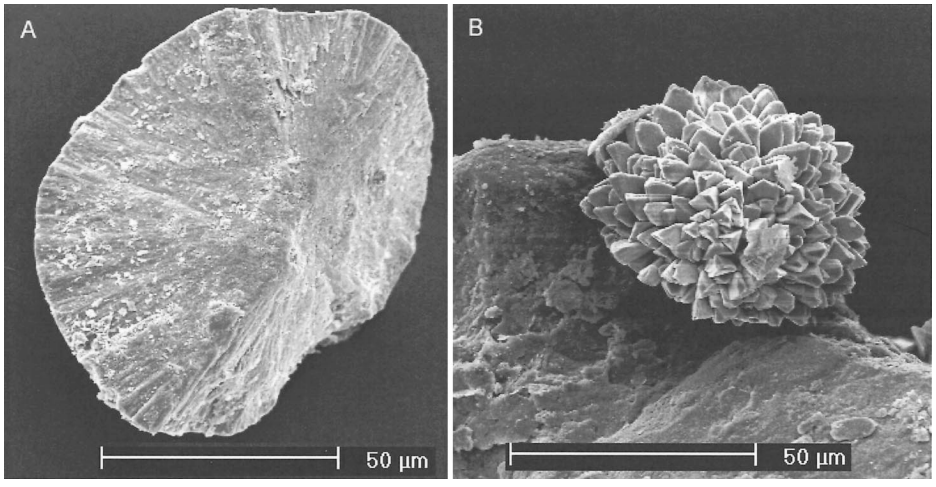

FIG. 7.—Scanning electron micrographs. **A**) Example of a fibro-radial calcite spherulite found associated with polysaccharides in a tropical soil. **B**) Vaterite cluster from a tropical soil showing a structure identical to those obtained in Figure 4J, M, and N. This vaterite cluster grew on a silica substratum in a biofilm rich in exopolysaccharides and amino acids.

xanthan solution is 1000x greater than water (water: 1 centipoise or cp at 20°C; xanthan 1.0%: 1042 cp). For 0.1% and 0.5% xanthan solutions, the viscosity is about 30 cp and 450–500 cp, respectively. This is consistent with the observations made by Buczynski and Chafetz (1991) who stated that the viscosity of the medium is the single most important control over the mineral precipitation.

All the amino acids tested in this study enhanced sphere formation. At high xanthan concentrations, amino acids induced vaterite precipitation with traces of calcite. The role of the carboxyl group is probably critical. This group shows a similar spatial configuration to the calcite lattice, and therefore shares important geometrical homologies with carbonate ions (Mitterer and Cunningham 1985; Addadi et al. 1990; Neumeier 1998). The influence of aspartic and glutamic acids on calcium carbonate crystallization has been studied extensively. These amino acids have been reported to induce mainly vaterite precipitation (Falini 2000; Manoli and Dalas 2001). Bacterial outer structures associated with peptidoglycan (homopolypeptide—polyglutamine in the case of *X. autotrophicus* and polyglutamic acid in the case of several *Bacillus* species—or proteins) often contain carboxyl and/or amide groups. This fact, combined with the results presented in Figures 4, 5, and 6, clearly demonstrate the influence bacterial outer structure composition can have on the morphology and mineralogy of bacterially induced calcium carbonate. This point should not be neglected in the interpretation of calcite cements and carbonate accumulations in terrestrial environments.

CONCLUSIONS

From the results presented in this paper, it seems likely that spherulitic calcite and/or vaterite crystals may indicate the presence of mucilaginous bacteria or biofilms at the time of formation (and probably other mucilage-producing organisms, e.g., cyanobacteria or fungi). The relative abundance of mineral species (calcite vs. vaterite) can be informative in determining the nature of the biofilm, i.e., if they contain polyaspartic acid or other polyamino acids. In terms of sedimentary petrology, these results question the origin of some cements found in terrestrial sediments that were previously attributed to purely physicochemical processes.

AKNOWLEDGEMENTS

The authors wish to thank Dr. T. Adatte for XRD analysis, N. Jeanneret, M. Vlimant, M. Leboeuf, and K. Verrecchia for their helpful advice during the work. Associate editor Hank Chafetz, Neva Çiftçioglu (NASA, Houston) and Jan Toporski (Carnegie Institution of Washington) greatly improved the first version of the manuscript. Editing by John B. Southard was greatly appreciated. This work is supported by the Swiss National Science Foundation, grant no. 2153–065174.01.

REFERENCES

Addadi, L., Berman, A., Moradial-Oldak, J., and Weiner, S., 1990, Tuning of crystal nucleation and growth by protein: Molecular interaction at solid–liquid interfaces in biomineralization: Croatica Chemica Acta, v. 63, p. 539–544.

Boquet, E., Boronat, A., and Ramos-Cormenzana, A., 1973, Production of calcite (calcium carbonate) crystals by soil bacteria is a general phenomenon: Nature, v. 246, p. 527–528.

Braissant, O., and Verrecchia, E.P., 2002, Microbial biscuits of vaterite in Lake Issyk-Kul (Republic of Kyrgyzstan)—Discussion: Journal of Sedimentary Research, v. 72, p. 944—946.

Braissant, O., Aragno, M., and Verrecchia E.P., 2002, Is the contribution of bacteria to terrestrial carbon budget greatly underestimated?: Naturwissenschaften, v. 89, p. 366–370.

Buczynski, C., and Chafetz H.S., 1991, Habit of bacterially induced precipitates of calcium carbonate and the influence of medium viscosity on mineralogy: Journal of Sedimentary Petrology, v. 61, p. 226–233.

Castanier, S., Le Métayer-Levrel, G., and Perthuisot, J.-P., 2000, Bacterial roles in the precipitation of carbonate minerals, *in* Riding, R.E., and Awramik, S.M., eds., Microbial Sediments: Heidelberg, Springer-Verlag, p. 32–39.

Castanier, S., Perthuisot, J.-P., Matrat, M., and Morvan, J.-Y., 1999, The salt ooids of Berre salt works (Bouche-du-Rhône, France): the role of bacteria in salt crystallisation: Sedimentary Geology, v. 125, p. 9–21.

Chafetz, H.S., 1986, Marine peloids: a product of bacterially induced precipitation of calcite: Journal of Sedimentary Petrology, v. 56, p. 812–817.

Decho, A.W., 1990, Microbial exopolymer secretions in ocean environments: Their role(s) in food webs and marine processes: Annual Review of Oceanography and Marine Biology, v. 28, p. 73–154.

Decho, A.W., 2000, Exopolymer microdomains as a structuring agent for heterogeneity within microbial biofilms, *in* Riding, R.E., and. Awramik, S.M., eds., Microbial Sediments: Heidelberg, Springer-Verlag, p. 1–9.

Dedek, J., 1966, Le carbonate de chaux: Louvain, Librairie Universitaire de Louvain, 351 p.

Dey, S., Basu Baul, T.S., Roy, B., and Dey, D., 1988, A new rapid method of air-drying for scanning electron microscopy using tetramethylsilane: Journal of Microscopy, v. 156, p. 259–261.

Ehrlich H.L., 1996, Geomicrobiology: New York, Marcel Dekker, Inc., 720 p.

Ehrlich, H.L., 1998, Geomicrobiology: its significance for geology: Earth-Science Reviews, v. 45, p. 45–60.

Falini, G., 2000, Crystallization of calcium carbonate in biologically inspired collagenous matrices: International Journal of Inorganic Materials, v. 2, p. 455–461.

Ferris, F.G., Shotyk, W., and Fyfe, W.S., 1989, Mineral formation and decomposition by microorganisms, *in* Beveridge, T.J., and Doyle, R.J., eds., Metal Ions and Bacteria: New York, Wiley, p. 413–441.

Folk, R.L., 1993, SEM imaging of bacteria and nanobacteria in carbonate sediments and rocks: Journal of Sedimentary Petrology, v. 63, p. 990–999.

Giralt, S., Julià, R., and Klerkx, J., 2001, Microbial biscuits of vaterite in Lake Issyk-Kul (Republic of Kyrgyzstan): Journal of Sedimentary Research, v. 71, p. 430–435.

González-Muñoz, M.T., Ben Chekroun, K., Ben Aboud, A., Arias, J. M., and Rodriguez-Gallego, M., 2000, Bacterially induced Mg-calcite formation: role of Mg^{2+} in development of crystal morphology: Journal of Sedimentary Research, v. 70, p. 559–564.

Holt, J.G., Krieg, N.R., Sneath, P.H.A., Staley, J.T., and Williams, S.T., 1993, Bergey's manual of determinative bacteriology: Philadelphia, Lippincott,Williams and Wikins, 787 p.

Kajander, E.O., and Çiftçioglu, N., 1998, Nanobacteria: an alternative mechanism for pathogenic intra- and extracellular calcification and stone formation: Proceedings of the National Academy of Science of U.S.A., v. 95, p. 8274–8279.

Kandler, O., König, H., Wiegel, J., and Claus, D., 1983, Occurrence of poly-γ-glutamic acid and poly-α-glutamine in the genera *Xanthobacter, Flexithrix, Sporosarcina* and *Planococcus*: Systematic and Applied Microbiology, v. 4, p. 34–41.

Krumbein, W.E., 1975, Biogenic monohydrocalcite spherules in lake sediments of Lake Kivu (Africa) and the Solar Lake (Sinai): Sedimentology, v. 22, p. 631–634.

Krumbein, W.E., 1979, Calcification by bacteria and algae, *in* Trudinger, P.A., and Swaine, D.J., eds., Biogeochemical Cycling of Mineral-Forming Elements: Amsterdam, Elsevier, p. 47–68.

Lal, R., Kimble, J.M., Eswaran, H., and Stewart, B.A., 2000, Global Climate Change and Pedogenic Carbonates: Boca Raton, Lewis Publishers, 305 p.

Mann, S., 2001, Biomineralization—Principles and Concepts in Bioinorganic Materials Chemistry: Oxford, Oxford University Press, 210 p.

Manoli, F., and Dalas, E., 2001, Calcium carbonate crystallization in presence of glutamic acid: Journal of Crystal Growth, v. 222, p. 293–297.

Mitterer, R.M., and Cunningham, R., 1985, The interaction of natural organic matter with grain surfaces: implications for calcium carbonate precipitation, *in* Schneidermann, N., and Harris, P.M., eds., Carbonate Cements: Society of Economic Paleontologists and Mineralogists, Special Publication 36, p. 17–31.

Neumeier, U., 1998, Le rôle de l'acivité microbienne dans la cimentation des beachrocks (sédiments intertidaux) [Thèse de doctorat es Science]: Genève, Université de Genève, 183 p.

Rivadeneyra M.A., Delgado G., Ramos-Cormenzana A., and Delgado R., 1998, Biomineralization of carbonates by *Halomonas eurihalina* in solid and liquid media with different salinities: crystal formation sequence: Research in Microbiology, v. 149, p. 277–287.

Rivadeneyra, M.A., Ramos-Cormenzana, A., Delgado, G., and Delgado, R., 1996, Process of carbonate precipitation by *Deleya halophila*: Current Microbiology, v. 32, p. 308–313.

Schultze-Lam, S., Fortin, D., Davis, B.S., and Beveridge, T.J., 1996, Mineralization of the bacterial surface: Chemical Geology, v. 132, p. 171–181.

Schultze-Lam, S., Harauz, G., and Beveridge, T.J., 1992, Participation of a cyanobacterial S layer in fine-grain mineral formation: Journal of Bacteriology, v. 174, p. 7971–7981.

Smarda, J., Smajs, D., Komrska, J., and Krzyzanek, V., 2002, S-layers on cell walls of cyanobacteria: Micron, v. 33, p. 257–277.

Sutherland, I.A., 2001a, The biofilm matrix—an immobilized but dynamic microbial environment: Trends in Microbiology, v. 9, p. 222–227.

Sutherland, I.A., 2001b, Biofilm exopolysaccharides: a strong and sticky framework: Microbiology, v. 147, p. 3–9.

Vali, H., McKee, M.D., Çiftçioglu, N., Sears, S.K., Plows F.L., Chevet, E., Ghiabi, P., Plavsic, M., Kajander, O.E., and Zare, R.N., 2001, Nanoforms: a new type of protein-associated mineralization: Geochimica et Cosmochimica Acta, v. 65, p. 63–74.

Verrecchia, E.P., Freytet, P., Verrecchia, K.E., and Dumont, J.-L., 1995, Spherulites in calcrete laminar crusts: biogenic $CaCO_3$ precipitation as major contributor to crust formation: Journal of Sedimentary Research, v. A65, p. 690–700.

Warthmann, R., Van Lith, Y., Vasconcelos, C., McKenzie, J.A., and Karpoff A.M., 2000, Bacterially induced dolomite precipitation in anoxic culture experiments: Geology, v. 28, p. 1091–1094.

Wiegel J., 1991, The Genus *Xanthobacter, in* Balows, A., Trüper, H.G., Dworkin, M., Harder, W., and Schleifer, K.H., eds., The Prokaryotes: New York, Springer-Verlag, p. 2365–2383.

Received 22 July 2002; accepted 13 November 2002.

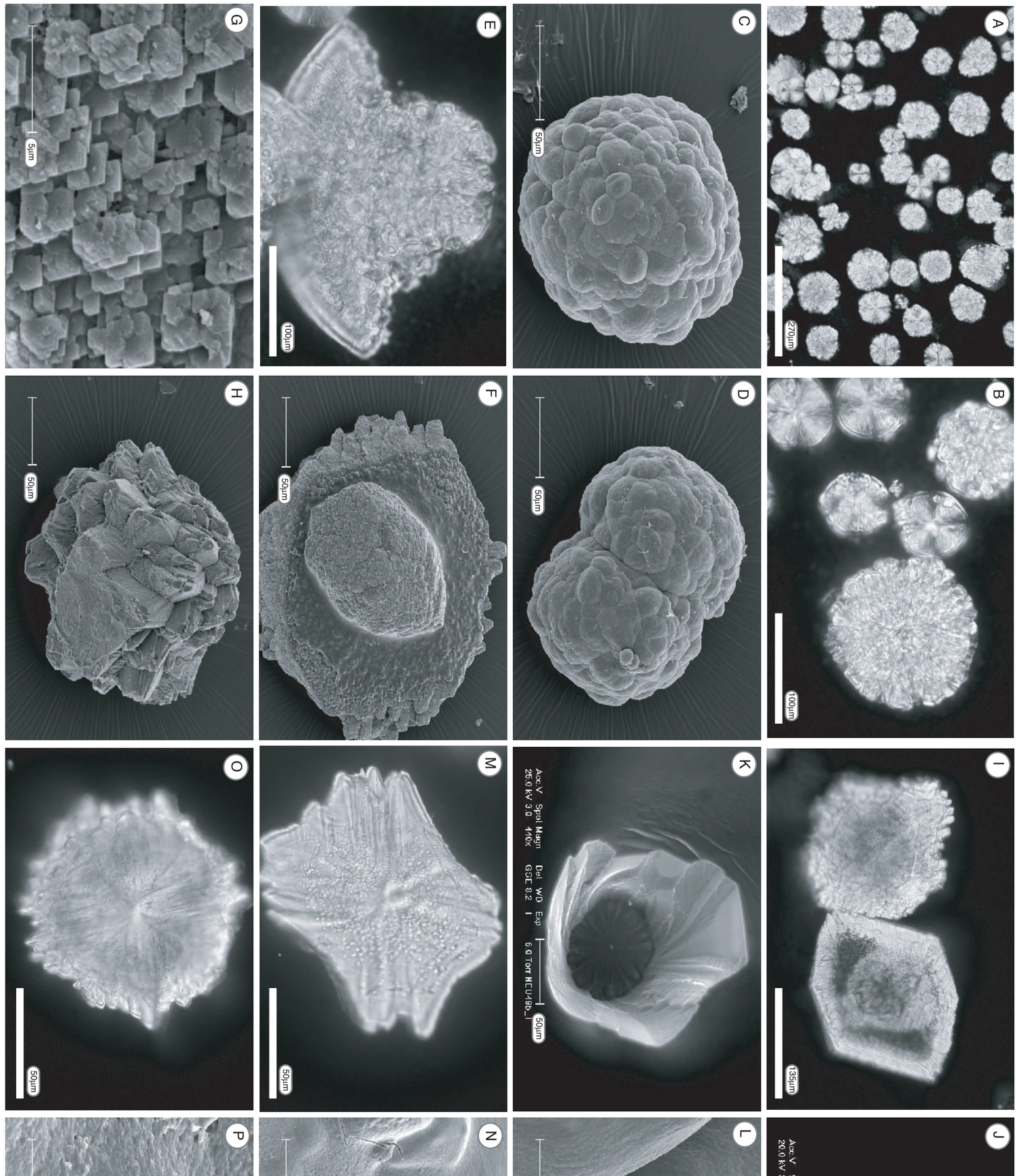
A
270µm
C
50µm
E
100µm
G
5µm
B
100µm
D
50µm
F
50µm
H
50µm
I
135µm
K
Acc.V Spot Magn Det WD Exp
25.0 kV 3.0 416x GSE 8.2 I 6.0 Torr NCU49b_
50µm
M
50µm
O
50µm
J
Acc.V Spot
20.0 kV 3.0
L
N
P

Blank

Gln

Glu

Asp

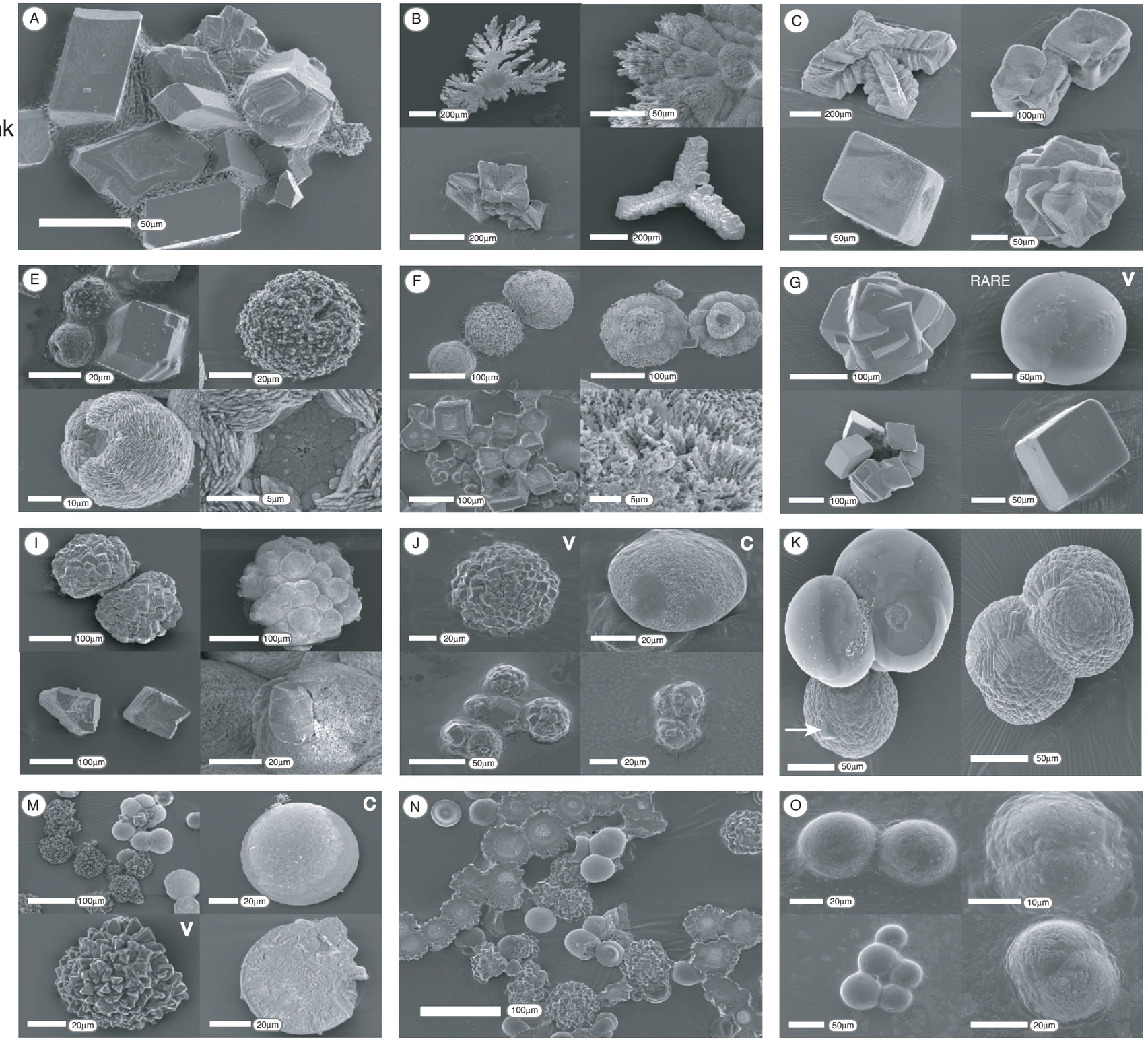

0.0%

0.1%

0.5%